



DOUBLER SYSTEM QUENCH DETECTION THRESHOLD

K.Koepke and P.Martin

January 25, 1982

I. INTRODUCTION

The purpose of this paper is to establish the quench detection threshold at which the Quench Protection Monitor must operate in order that the numerous components of the Doubler superconducting magnet system are not damaged during a quench. A method is presented which, given the location of the quench and the quench detection threshold, predicts the peak temperature that occurs in the superconductor as a function of quench current. A comparison of the predicted quench behavior with quench data obtained at the B12 Test Facility shows good agreement, indicating that the method can be useful in calculating the quench behavior in geometries which as yet have not been measured or are difficult to measure.

II. DOUBLER QUENCH PROTECTION SYSTEM

The complexity of the Doubler refrigeration system, beam loss, and the small short sample safety factor inherent in the Doubler magnet design virtually guarantee that quenches will occur during the operation of the superconducting accelerator. Therefore, the Quench Protection System must tolerate repeated quenches without damage to the superconducting system.

A section of the Doubler magnet power circuit is shown in Fig. 1. Each magnet cell (typically eight dipoles and two quadrupoles) constitutes one quench protection unit (QPU). Each QPU is further divided into upper and lower voltage monitoring and quench bypass switch (QBS) units. In the absence of a quench, the ramp current driven by the power supplies flows through the main bus and magnet coils. The main bus current and the QPU voltages (voltage difference between voltage taps) are continuously monitored at a 60 cycle rate by the microprocessor-based quench protection monitors (QPM). A QPM recognizes a quench in a QPU when the measured QPU voltage differs from the expected inductive voltage $L \frac{dI}{dt}$ by an amount equal to the quench detection threshold. The QPM responds to this quench signal as follows.

1. The magnet power supplies are switched to bypass.
2. The dump thyristors are turned off which switches the dump resistors into the magnet circuit.

3. The QBS thyristor gates are forward biased.
4. One heater is energized in each dipole of the cell that contains the quench.

Neglecting the effects of the quenching magnets - true only if a small fraction of the Doubler magnets are quenching - the ramp current now begins to decay exponentially with a 12 second time constant determined by the series magnet inductance and the series dump resistance. There is no bypass current through the QBS thyristors at this time as the decaying ramp back biases the QBS.

Firing the heaters in the dipoles of the quenching cell has caused a substantial fraction of their coils to become normal. Within a fraction of a second, the increasing resistive voltage equals the inductive bias due to the decaying ramp and the QBS start to conduct. The current i_Q through the quenching magnets now satisfies the equation

$$\frac{L}{(R_Q+R)} \frac{di_Q}{dt} + i_Q = \frac{IR}{R_Q+R} e^{-t/12} + \frac{V}{(R_Q+R)} \quad (1)$$

where L is the QPU inductance, R_Q the quench resistance, R the sum of the safety lead and QBS cable resistances, V is the QBS thyristor voltage and I is the initial magnet current. To prevent the superconductor from overheating, the time dependant time constant

$$T_Q = \frac{L}{R_Q+R} \quad (2)$$

must be much less than the 12 second time constant of the decaying ramp.

The magnet current i_Q must be determined experimentally. It has been measured at B12 and is plotted in Fig. 2 starting 1 second before the QPM recognizes the quench.

Typical of the quench related failures experienced during the operation of the superconducting magnet system at B12 are the overheating of the superconducting cable due to ohmic heating, magnet turn-to-turn or turn-to-ground dielectric failures, and ruptures of the cryogenic system. A spectacular example combining all three of the above follows:

First, the normal region of the superconducting cable overheats and melts. Second, the plasma which forms to conduct the current remaining in the inductive circuit shorts to ground and finally, burns a hole into the cryostat.

The possibility of a ruptured cryostat due to a quench-produced pressure pulse has been discussed in another paper.* The possibility of a dielectric failure to ground has been reduced by the decision to double the number of dump circuits while simultaneously correcting known failure-prone insulation areas in the magnet system. Except in prototype magnets, the turn-to-turn dielectric breakdown rate has been small and in principle, could be reduced further by energizing both heaters in the dipoles simultaneously. The possibility of overheating cables and how this relates to the quench detection threshold constitutes the remainder of this paper.

III. QUENCH TEMPERATURE, QUENCH VOLTAGE, AND QUENCH MIITS

The upper thermal limit for Doubler superconducting cable during a quench has been set at the melting point of solder, 453K. At this temperature the internal and intercoil splices, along with the Stay-Brite coating of its strands, will melt. It is difficult to measure the hottest point of the quenching superconducting circuit directly. Thermometers imbedded within a magnet are in general too large and presuppose a knowledge of the initial location of every quench, while a measurement of the total magnet resistance yields an average temperature. We therefore estimate the temperature in a quenching conductor by integrating the net energy deposition rate for an infinitesimal conductor section starting from the time when the section goes normal.

The conservation of energy equation for a conductor of length $d\ell$, carrying a current I , normal to its cross section A , can be integrated to yield the form

$$\int_0^t I^2 dt = A^2 \mu \int_{T_c}^T \frac{c}{\rho} dT + \frac{A}{d\ell} \int_0^t \frac{w}{\rho} dt \quad (3)$$

where the density μ , specific heat c , and resistivity ρ , of the cable are known over the temperature range of interest. The quantity w represents the sum of the transverse and longitudinal power leaving the volume $Ad\ell$. The integral

$\int_0^t I^2 dt$, usually evaluated in units of $10^6 A^2 s$ (MIITS), uniquely determines the conductor temperature T at time t . In the case

*UPC-154

of the Doubler superconducting cable, quenches at currents of 4kA or greater approximate adiabatic ohmic heating. For lower quench currents, an estimate of w in Eq. (3) must be made or the relationship of temperature to MIITS can be determined experimentally.

The results of such an experiment performed by M.Kuchnir¹ in the short sample test fixture are reproduced in Figs. 3 and 4. The temperature of a quenching cable was measured by means of a known temperature-resistance curve. Quenches were started at one end of the cable with a heater. The cable voltage was monitored as a function of time at discrete fixed currents with a voltage tap separation of 17 cm to minimize the difference between the average and peak temperatures.

Figure 3 plots the quench voltage measured as a function of time. The time $t=0$ was defined as the point at which the quench voltage is just detectable within the background noise and represents the time when the cable closest to the heater starts to go normal. By relating the cable voltage to average temperature and time to MIITS, a map of average temperature vs MIITS is calculated (Fig. 4). The relationship of peak temperature to average temperature is derived in Appendix A. Note that as the quench current approaches 4kA, the spacing between individual curves decreases as they approach the adiabatic limit. The 7 MIIT cable limit at 4kA, first established by R.Flora in a hairpin experiment,² is also confirmed.

The quench velocity can be extracted from this experiment because the resistivity of the copper in the Doubler cable is approximately constant over the 10K to 30K temperature range. This results in a linear quench voltage growth with time until all of the cable is above the critical temperature. Then the quench voltage growth stops until the cable under the heater reaches 30K.

Figure 5 plots the quench velocities obtained by this method for several sections of Doubler cable. Note that this velocity applies only to quenches propagating in cables outside of coils and at zero magnetic field. Quenches that originate within a coil are dominated by transverse propagation and grow much more rapidly.

The quench voltage versus time for longer cables outside of coils can be extracted from the data of Fig. 3 and Fig. 5. If $T(I)$ is the time that a quench at current I requires to travel 17 cm, then the quench voltage $V(I,nT)$ for an infinite conductor length at time nT equals

¹Progress Report on Quench Capacity of Energy Saver Superconducting Cable, November 17, 1980

²TM-809

$$V(I, nT) = \sum_{\alpha=1}^n v(I, \alpha T) \quad n=1,2,\dots \quad (4)$$

$$T = T(I) = .17/.36I^2$$

where $v(I, \alpha T)$ is the quench voltage measured across a 17 cm section of cable at time αT and is given in Fig. 5. Quench voltages for times other than multiples of T can be obtained by interpolation and are given in Fig. 6. For quenches traveling in both directions, the voltages in Fig. 6 must be doubled. Conductors of finite lengths can be treated by subtracting from the voltage of Fig. 6 that voltage that would occur in the non-existent continuation of the finite cable. Doubled cables are equivalent to a single cable at half current.

IV. QUENCH DETECTION THRESHOLD

The discussion of the previous section shows that if we wish to limit the peak cable temperature to 453K for quenches that start outside of magnet coils, the MIITS during the quench must be maintained below 7-12 MIITS depending on current. Although the temperature-MIITS functional dependence of Fig. 4 is strictly valid only for conductors outside of coils, quenches at 4kA approximate adiabatic ohmic heating which forces us to set an upper limit of 7 MIITS for 4kA coil quenches also. For coil quenches below 4kA, a reasonable maximum MIITS assumption ranges somewhere between the 7 MIITS adiabatic limit and the values of Fig. 4.

For convenience, the total quench MIITS are split into the MIITS that accumulate prior to quench detection $M(t<0)$ and the MIITS that occur after quench detection $M(t>0)$. Experimental results at B12 indicate that $M(t>0)$ is a function of the quench current and approximately independent of quench origin and quench detection threshold. This is a consequence of the normal zone resistance created by four dipole heaters rapidly dominating the total quench resistance. $M(t>0)$ can be obtained from Fig. 2 and is plotted in Fig. 7.

$M(t<0)$ is a strong function of quench current, quench origin and quench detection threshold. In the case of a spontaneous coil quench or a dipole heater induced quench, the rapid rise in quench voltage minimizes the time error of the quench onset determination. The quench onset time is masked by the noise level present in the QPM voltage monitors. $M(t<0)$ data for this type of quench are plotted in Fig. 7. The data represents quenches detected at a 5.0V quench detection threshold. Note that even at this elevated quench threshold, the $t<0$ MIITS are small over the entire quench current range measured and that the total quench MIITS are safely below the MIITS that represent our 453K thermal limit.

Quenches beginning outside magnet coils are characterized by a very slow growth of the quench voltage. Not only are the MIITS prior to quench detection large, but the determination of the start of a quench is more difficult. Possible locations for quenches outside of magnet coils are inter-magnet splices and the long sections of superconducting cable in spool pieces, bypass sections, turnaround boxes and feedcans. The failure of a prototype spool piece which did not have doubled cables, showed that a 5V quench detection threshold was not able to protect superconducting cables outside magnet coils.

In the cases where the QPM as implemented is incapable of establishing the start time of the quench, we utilize the data in Figs. 4, 6, and 7 to calculate the required quench detection threshold. The worst assumption for a quench outside a coil is that it starts in a single cable (not doubled) and propagates in one direction only. For this type of quench, the quench detection thresholds that result in a peak conductor temperature of 453K have been calculated and are listed in Table I. The parameter uncertainties contained in the Table are discussed in Appendix B.

The ultimate test of the validity of this calculation is a comparison of the predicted voltage with the quench voltage measured at B12. These comparisons are covered in the next two sections.

TABLE I

QUENCH VOLTAGE THAT LIMITS QUENCH TEMPERATURE TO 453K

Current (kA)	M(t>0) (10 ⁶ A ² s)	M(453K) (10 ⁶ A ² s)	M(t<0) (10 ⁶ A ² s)	Δ t (sec)	Threshold Volts
1	1.15±.25	11.6±.27	10.45±.38	10.45+.38 -.40	3.0±.4
2	3.05±.3	8.4±.20	5.35±.36	1.34+.09 -.11	1.6±.4
3	4.25±.35	7.5±.18	3.25±.39	.361+.043 -.060	.68±.3
4	4.7±.5	7.0±.16	2.30±.52	.144+.053 -.049	.5±.32

V. QUENCHES INDUCED AT SPLICES BETWEEN MAGNETS

Two series of quench tests were performed using special heaters located at the splices between a quadrupole and a dipole. In the first series, the splice between the coil of the quad and coil of the dipole was quenched. In the second series of tests, the bus splice was quenched. The quench evolution during these tests is shown in Figs. 8, 9, 10 and 11.

At 1kA, the quenches propagate into the coil before the quench voltage has reached 0.5V. In the case of the coil-splice quench, transverse quench propagation causes a sudden departure from the expected growth pattern. In the bus-splice quench, transverse propagation, although retarded in time by the extra cable length, quenches the coil portion which then grows rapidly to the quench threshold. Also, the bus signal increases somewhat more rapidly during this time, possibly due to overheating with the quench starting resistor. The solid lines represent the predicted quench evolution obtained from Fig. 6, assuming quench propagation in two directions. The time scale of the B12 data is shifted to agree with the predicted time at levels of .07V to .15V.

At higher currents, the coil-splice and bus-splice quenches are more similar. In the figures, the solid line is the prediction for quench propagation in two directions while the dashed line is the prediction for propagation in one direction. The two curves are again adjusted in time so that they are equal at roughly .5V. The 2kA and 3kA quenches would tend to indicate two-directional growth while the 4kA quenches indicate growth in one direction. In all cases, there is probably propagation in both directions. However, propagation in one direction is retarded slightly by the splice itself where the quench velocity is down by a factor of 4 from the single cable.

The following table lists the MIITS before and after quench detection for the splice-induced quenches. The uncertainties shown for $M(t < 0)$ reflect the uncertainty of propagation in one or two directions. The uncertainties shown for $M(t > 0)$ are based upon the observed spread in MIITS at that quench current.

TABLE II

Current (kA)	M(t<0) (10 ⁶ A ² s)	M(t>0) (10 ⁶ A ² s)	Total MIITS (10 ⁶ A ² s)
1.0 (coil)	2.5-3.5	0.9-1.4	3.4-4.9
1.0 (bus)	3.5-4.5	0.9-1.4	4.4-5.9
2.0 (bus or coil)	2.8-3.5	3.0-3.1	5.8-6.6
3.0 (bus or coil)	2.2-2.9	3.9-4.6	6.1-7.5
4.0 (bus or coil)	1.9-2.4	4.2-5.2	6.1-7.6

VI. QUENCHES INDUCED NEAR A QUENCH STOPPER

A resistor mounted on the double-lead bus of a spool piece was used to induce quenches at 2, 3 and 4kA. The double-lead was attached on one end to a quench stopper and on the other end to a quadrupole bus. The location of the resistor along the double-lead is only known to ± 10 cm. The calculations assume that the resistor is 36cm from the quench stopper and 53cm from the splice.

The data are shown in Figs. 12, 13 and 14 along with the predictions of our model. Again, the zero point of the time scale is derived from the model. As in the previous section, the calculation of the MIITS prior to quench detection must rely upon the model. The MIITS in the single and double cables are presented in Table III.

For quenches starting in a double cable and propagating into a single cable, the double cable, which can take four times the MIITS of the single cable, is very safe. In addition, the voltage developed on the double cable reduces the voltage that the single cable must develop to reach the detection threshold. This in turn reduces the MIITS for the single cable. In these quenches, the MIITS for the single cable was reduced by about .5 MIIT.

In order to reduce the noise present in the experimental data, the data was processed as follows:

The determination by the QPM of whether or not a quench has occurred is based upon the simultaneous measurements of the voltage and dI/dt . The signals are integrated, then sampled at 60Hz by the QPM and stored in a circular buffer. Before comparison, the voltage and dI/dt signals are averaged (with unequal weighing) with the previous two samples in order to reduce the noise.

The residual noise on the comparison signal is at the level of 100-200mV, most of which is common to all cells. This indicates that its source is the dI/dt signal. Because the noise is common to all cells, and only one cell is quenching, subtracting the average of the non-quenching signals from the quenching ones for each line cycle sample reduces the noise substantially. All of the data of this section and the previous section have had this subtraction performed.

VII. SUMMARY

The content of the previous sections indicates that a quench detection threshold of 5.0V will protect quenching coils over the entire Doubler current range. In order to protect the

TABLE III

Double Cable: t_D is the time that the quench takes to reach the end of the double cable.

t_S is the time from start of quench in single cable to the time when the voltage reaches the quench detection threshold (0.5V).

Current (kA)	t_D (sec)	t_S (sec)	$M_D(t < 0)$ ($10^6 A^2 s$)	$M_D(t > 0)$ ($10^6 A^2 s$)	Total MIITS ($10^6 A^2 s$)
2	1.5	.9	9.6	3.0-3.1	12.6-12.7
3	.67	.26	8.4	3.9-4.6	12.3-13.0
4	.37	.12	7.7	4.2-5.2	11.9-12.9

Single Cable:

Current (kA)	t_S (sec)	$M_S(t < 0)$ ($10^6 A^2 s$)	$M_S(t > 0)$ ($10^6 A^2 s$)	Total MIITS ($10^6 A^2 s$)
2	.9	3.6	3.0-3.1	6.6-6.7
3	.26	2.3	3.9-4.6	6.2-6.9
4	.12	1.9	4.2-5.2	6.1-7.1

cable outside of the coils, a detection threshold of as low as 0.5V should be used for currents above 2kA. Although the QPM at B12 has been refined to the point where it operates near a 0.5V level, we must assume that the larger tunnel magnet circuit is likely to contain higher noise levels. A partial solution to this problem is to operate each QPU at as low a threshold as possible, yet high enough so that false quenches do not occur too frequently. In addition, special voltage monitors could be implemented, analogous to the protection used on power leads, to protect those regions most likely to require higher sensitivity.

The consequences of operating at a 1.0V level are also of interest. At this detection level, mean peak temperatures of $550K \pm 100K$ and $660 \pm 200K$ are calculated for unidirectional quenches at 3kA and 4kA respectively. Although the Stay-Brite coating of the cable will melt, this is not critical as eddy current effects are unimportant outside of the coils. Any cable splice near such a quench should survive because of its larger cross section. The dielectric strength of Kapton degrades gradually with temperature, but at 600K is only reduced by a factor of 3 relative to room temperature (Fig. 15). The NbTi superconductor should also survive up to at least 600K as the splices are routinely soldered at this temperature.

A temperature of 860K is possible for a 4kA quench with a 1.0V threshold. At this temperature, the cable would remain intact - copper melts at 1356K - but the Kapton insulation would fail. Fortunately, unidirectional quench propagation in single conductors is extremely unlikely. This type of quench can only result from a faulty splice and has never occurred outside of coils unless started with a heater. The types of quenches which are likely start either at the power leads or at the quench stoppers. These regions contain double cable which can tolerate four times the MIITS of a single cable.

APPENDIX A

PEAK TEMPERATURE VERSUS AVERAGE TEMPERATURE

In the adiabatic approximation, Eq. (3) of page 3 can be integrated over a temperature range where ρ and c are known. If we assume that the cable resistance per unit length has the form

$$\rho = A(\alpha T - \beta) \Omega/\text{cm} \quad T \geq 273\text{K} \quad (\text{A1})$$

and that the specific heat is constant over this temperature, then $\rho(T)$ satisfies the following function

$$\rho(T) = (273)e^{\theta m} \quad T \geq 273\text{K} \quad (\text{A2})$$

$$\theta = \alpha/A\mu c$$

$$m = M(T) - M(273\text{K})$$

Next we average $\rho(T)$ over the cable length L and express the maximum resistance $\rho_{\max}(T)$ in terms of the average resistance $\overline{\rho(T)}$

$$\overline{\rho(T)} = \frac{1}{L} \int_0^L \rho(T) dx$$

$$\rho_{\max}(T) = \theta m' (1 - e^{-\theta m'})^{-1} \overline{\rho(T)} \quad (\text{A3})$$

$$m' = m(L) - m(0)$$

At a current of 4kA and for a length of 17 cm, we obtain

$$m' = 0.5 \text{ MIITS}$$

$$\rho_{\max}(T) = 1.1 \overline{\rho(T)} \quad (\text{A4})$$

$$\Delta T = T_{\max} - \bar{T} = .1 \bar{T}$$

From Fig. 4 we obtain an expression for the average temperature as a function of MIITS

$$\bar{T} = 273 e^{-.424m} \quad (\text{A5})$$

$$m = M(T) - M(273)$$

$$T \geq 273\text{K}$$

$$\Delta T = \bar{T}(-.424\delta m) \quad (A6)$$

$$.1 = -.424 (\delta m)$$

$$\delta m = -.24 \text{ MIITS}$$

The 4kA MIITS plotted in Fig. 4 at an average temperature of 453K must therefore be reduced by 0.24 MIITS if we wish to relate MIITS to a peak temperature of 453K.

APPENDIX B

M(t>0)

The uncertainties listed are the extreme range of MIITS measured for the four half-cells at B12.

M(453K)

The MIITS taken from Fig. 4 were reduced by 0.24 MIITS to compensate for temperature averaging. At currents below 3kA, this subtraction is somewhat arbitrary.

An error estimate of M(453K) follows:

- A. A superconducting cable consists of 23 strands, each with a diameter of .0268"±.0003". This results in an uncertainty in the square of the cable area of 1% if the individual strand errors are added in quadrature. The cable MIIT capacity has an area squared dependence. The total uncertainty of a measurement in MIITS (1%) applied to an arbitrary cable in the tunnel (another 1%) is therefore 1.4%.
- B. The average temperature - MIIT dependence of Fig. 4 was obtained from Fig. 3 by relating the voltage V of the ordinate to temperature T; the time of the abscissa to MIITS.

Ordinate uncertainty:

$$V = IR \quad (B1)$$

$$\frac{dV}{V} = \frac{dI}{I} + \frac{dR}{R} \quad (B2)$$

$$R = \alpha T - \beta \approx \alpha T \quad T > 400K \quad (B3)$$

$$\frac{dR}{R} = \frac{d\alpha}{\alpha} + \frac{dT}{T} \quad (B4)$$

$$\frac{dT}{T} = \frac{dV}{V} - \frac{dI}{I} - \frac{d\alpha}{\alpha} \quad (B5)$$

Abscissa uncertainty:

The average temperature - MIIT dependance has the form

$$\bar{T} = \bar{T}_0 e^{\theta m} \quad (B6)$$

$$m = M(\bar{T}) - M(\bar{T}_0)$$

$$200 \leq T \leq 500K$$

If we assume that the time measurement is without error, then

$$\frac{d\bar{T}}{\bar{T}} = 2\theta M(\bar{T}) \frac{dI}{I} \quad (B7)$$

and the overall error in $\frac{d\bar{T}}{\bar{T}}$ is

$$\frac{d\bar{T}}{\bar{T}} = \frac{dV}{V} + (2\theta M(\bar{T}) - 1) \frac{dI}{I} + \frac{d\alpha}{\alpha} \quad (B8)$$

where the correlation of the $\frac{dI}{I}$ -terms is explicitly shown.

The total uncertainty in \bar{T} is

$$\frac{d\bar{T}}{\bar{T}} = \left[\left(\frac{dV}{V} \right)^2 + (2\theta M(\bar{T}) - 1)^2 \left(\frac{dI}{I} \right)^2 + \left(\frac{d\alpha}{\alpha} \right)^2 \right]^{\frac{1}{2}} \quad (B9)$$

$$\left| \frac{dV}{V} \right| \approx .01 \quad \left| \frac{dI}{I} \right| \approx .01 \quad \left| \frac{d\alpha}{\alpha} \right| \approx .02$$

Current (kA)	θ	$M(\overline{453})$ (MIIT)	$\frac{d\bar{T}}{\bar{T}}$	dm (MIIT)
1	.28	11.8	.06	.21
2	.35	8.6	.055	.16
3	.38	7.7	.053	.14
4	.42	7.2	.055	.13

The uncertainty dm was obtained from the equation

$$\frac{d\bar{T}}{\bar{T}} = \theta dm \quad (B10)$$

Finally, the quantity $M(453)$ is obtained from the equation

$$M(453) = M(\overline{453}) - .24 \pm [(.014 M(\overline{453}))^2 + (dm)^2]^{\frac{1}{2}} \quad (B11)$$

Δt

The uncertainties in Δt are primarily due to the uncertainties in $M(t>0)$ and $M(453)$ which are added in quadrature. An additional .017 seconds is subtracted from this sum because the QPM samples the quench voltage at 60 Hz.

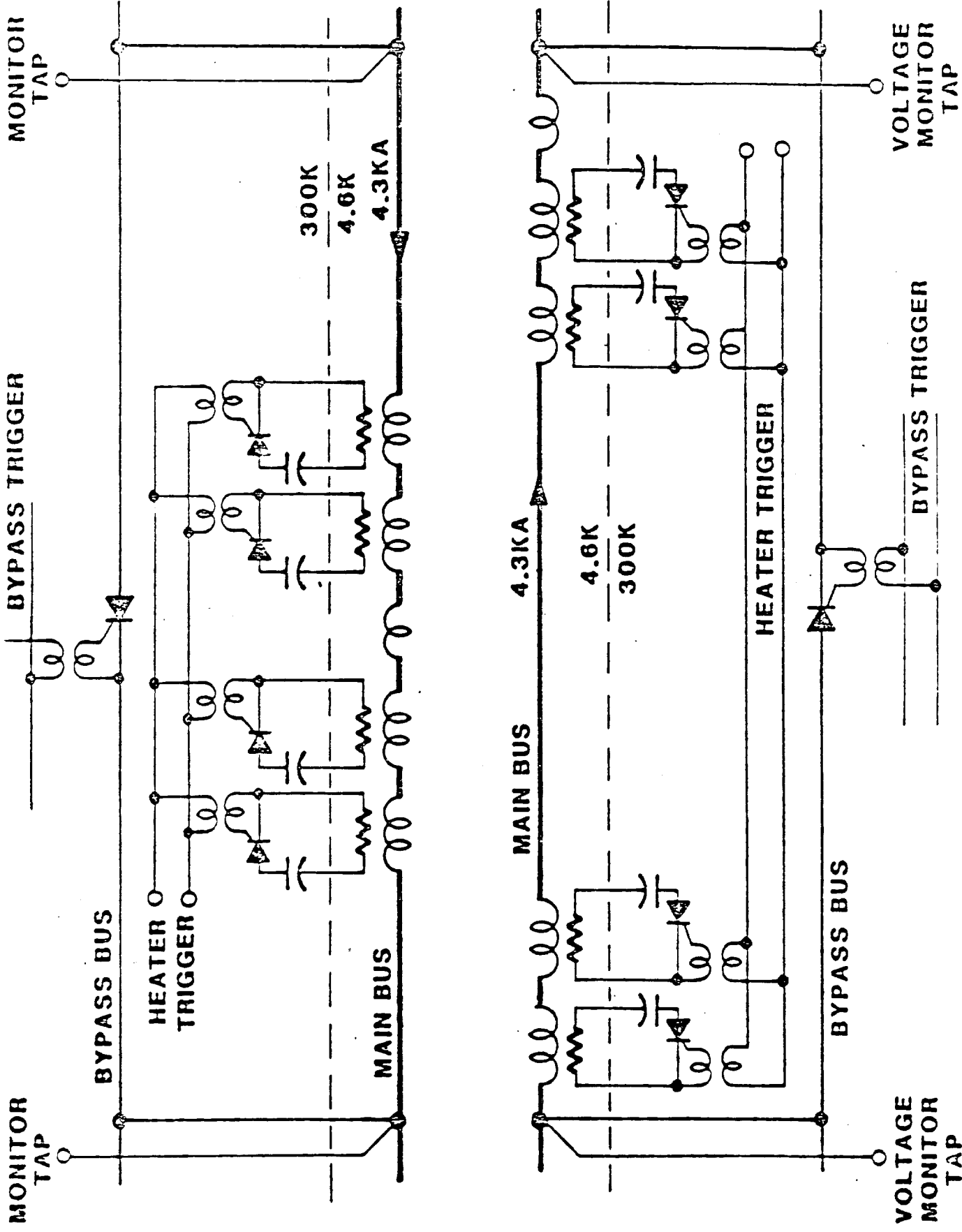


FIG. 1 QUENCH PROTECTION UNIT

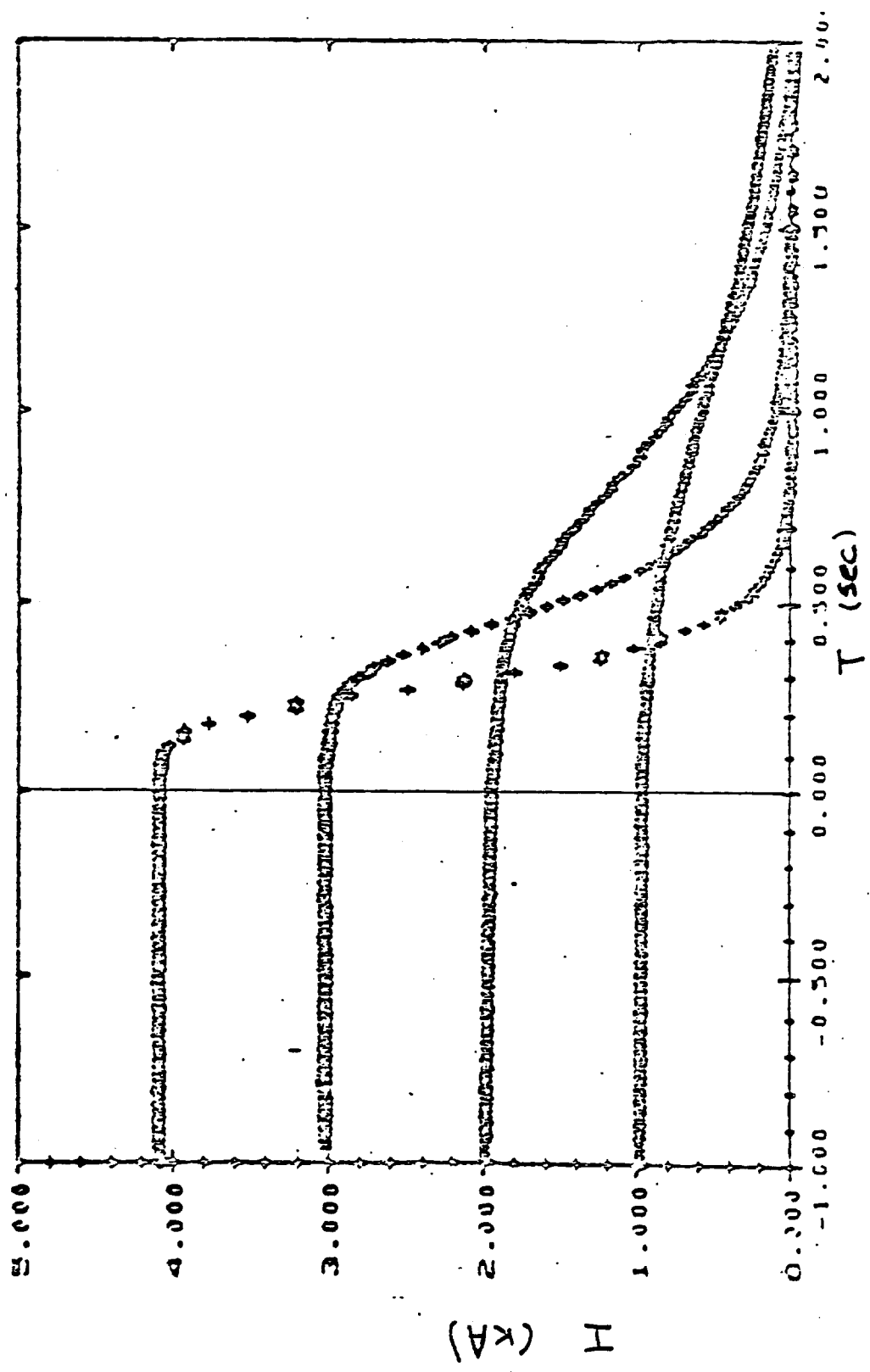
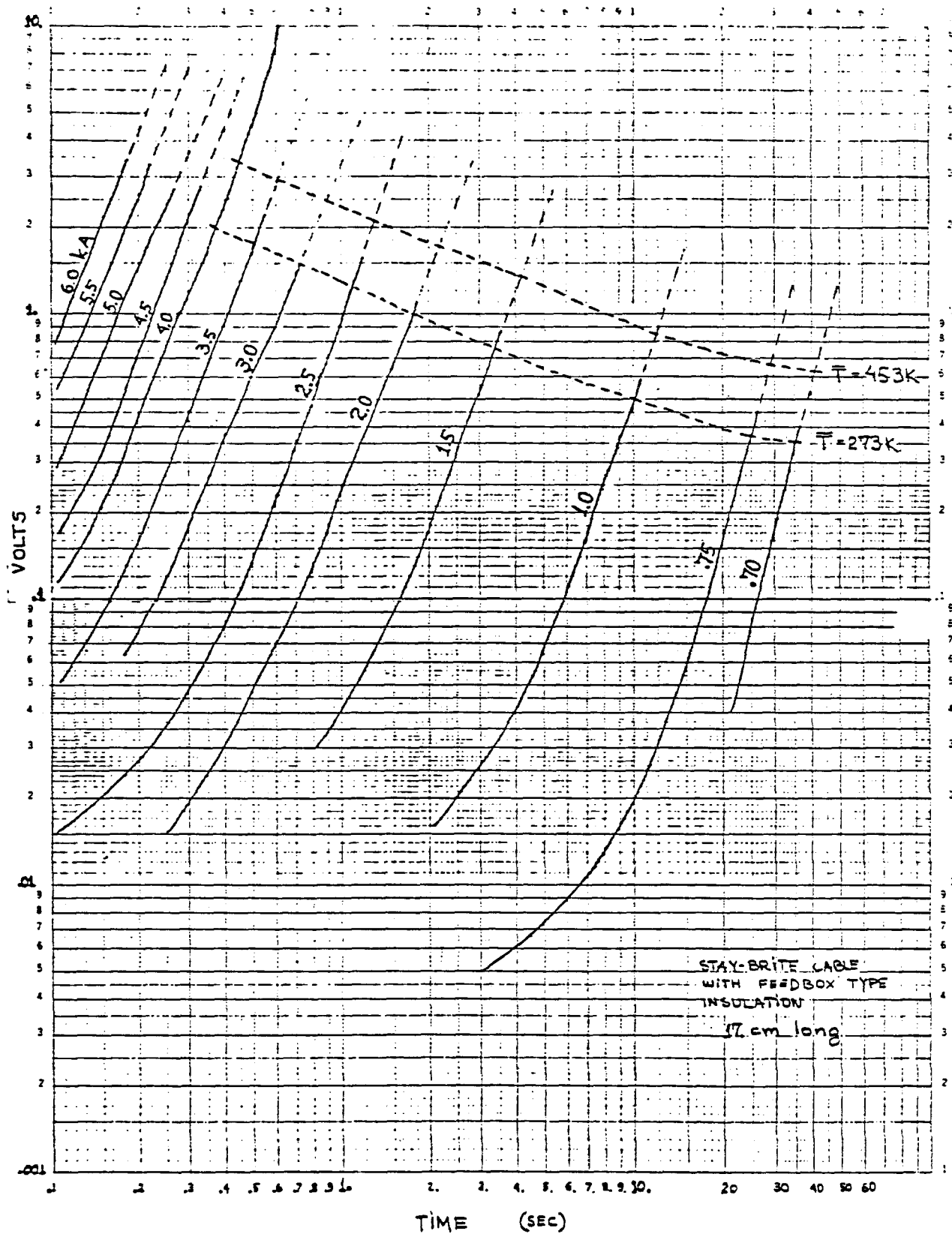


Fig 2. Magnet Current During a Quench



STAY-BRITE CABLE
WITH FEEDBOX TYPE
INSULATION
57 cm long

Fig. 3. Quench voltage development.

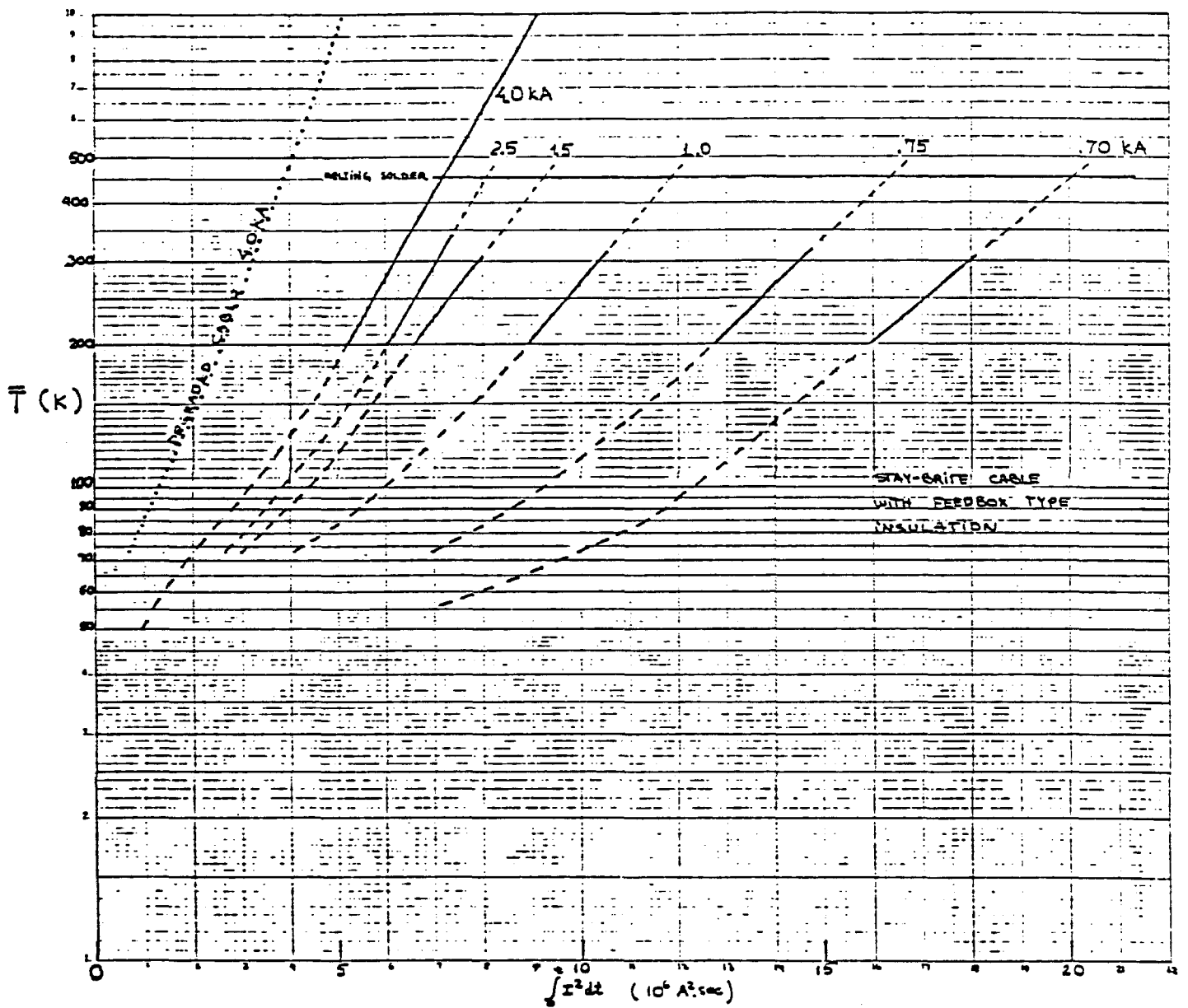


Fig. 4. Maximum average temperature as function of Miits.

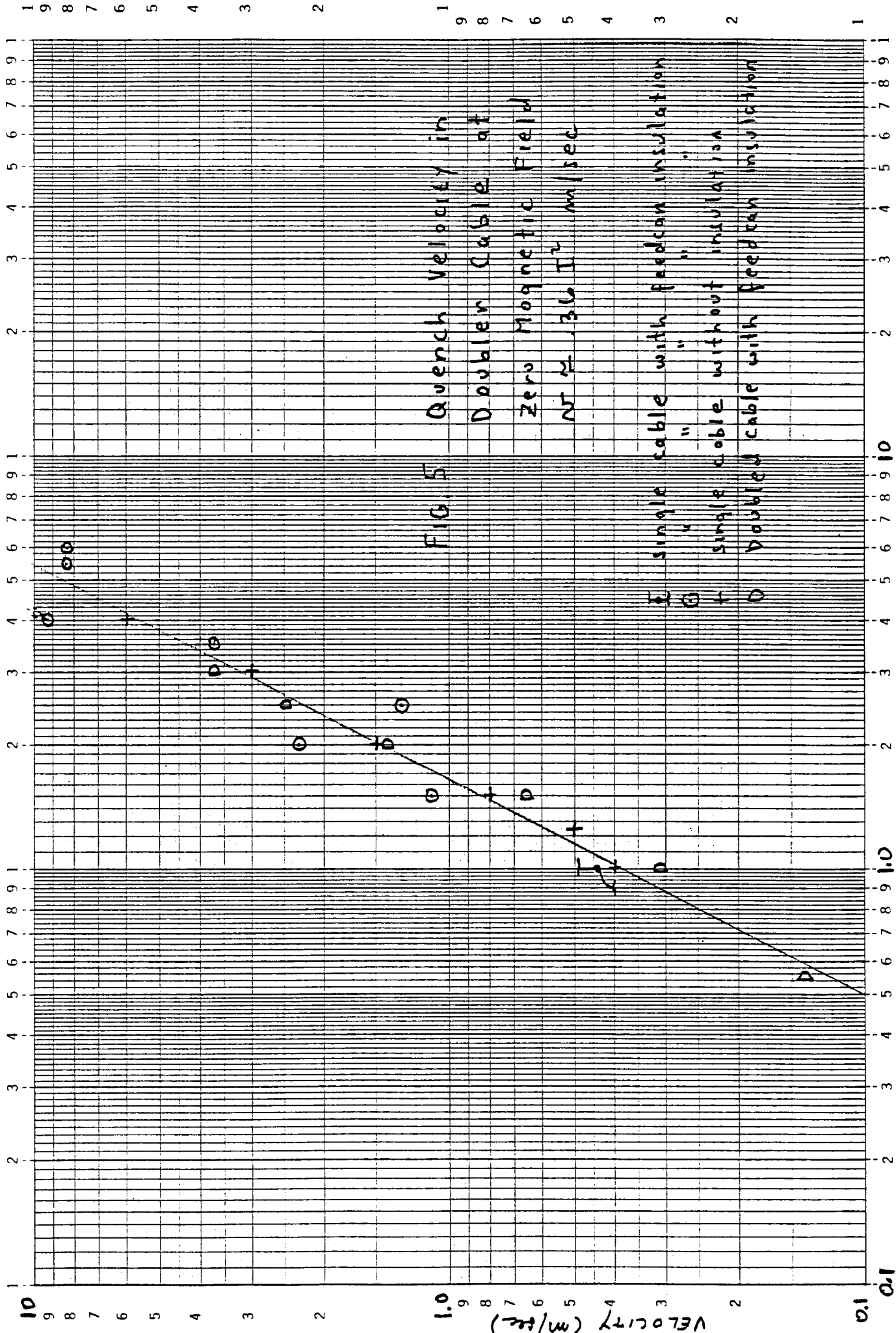
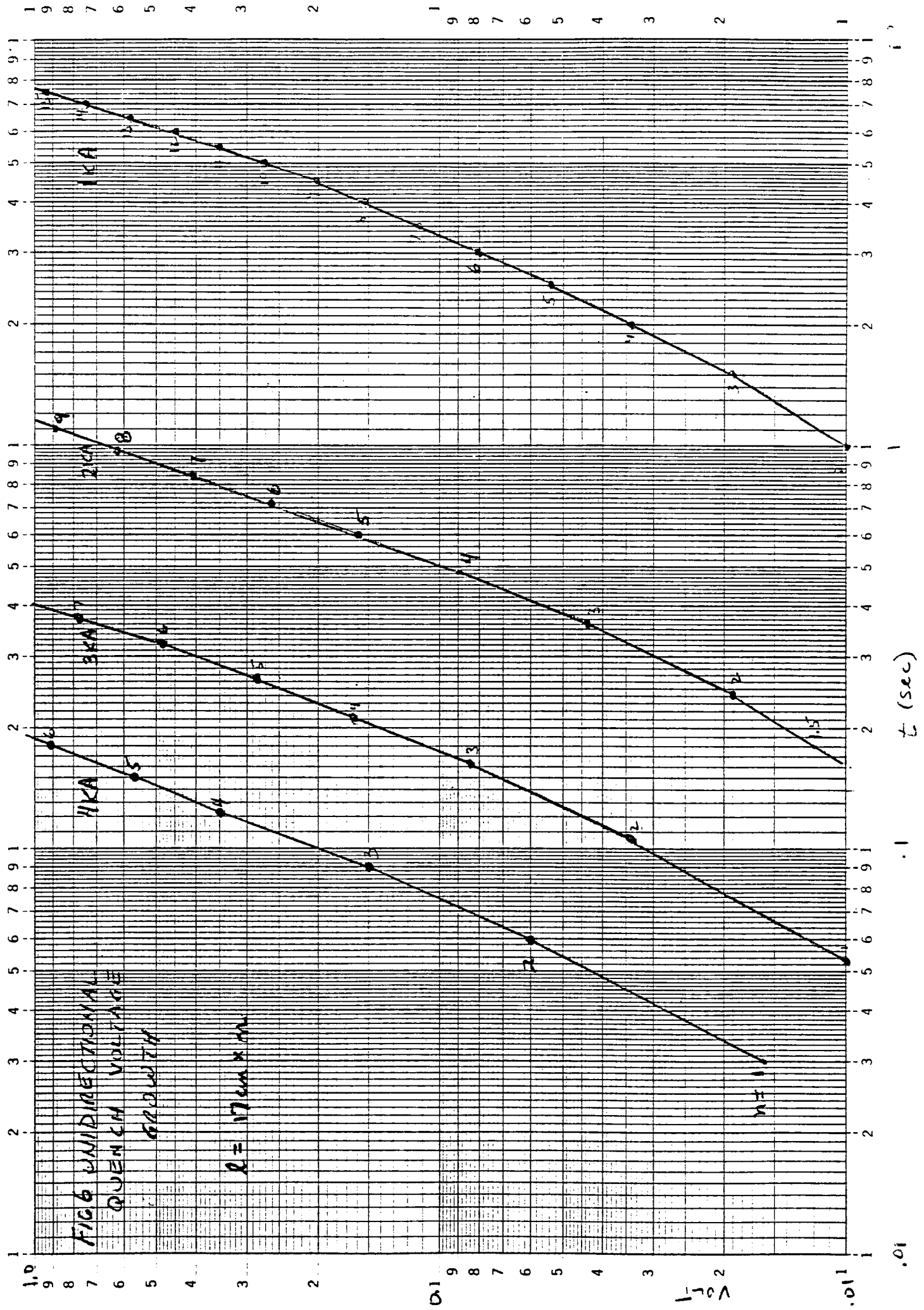


FIG. 5 Quench Velocity in
 Doubler Cable at
 Zero Magnetic Field
 $v \approx 136 I^{-1/2}$ m/sec

□ single cable with feedcan insulation
 ○ " " " " " "
 △ single cable without insulation
 ○ " " " " " "
 ○ Doubled cable with feedcan insulation

CURRENT (kA)

VELOCITY (m/sec)



QUENCHES INDUCED WITH SPARE HEATER
IN MAGNET COIL

- $M(t < 0)$ QUENCH DETECTION THRESHOLD = 5 V
ERROR BARS REPRESENT ONE LINE CYCLE UNCERTAINTY

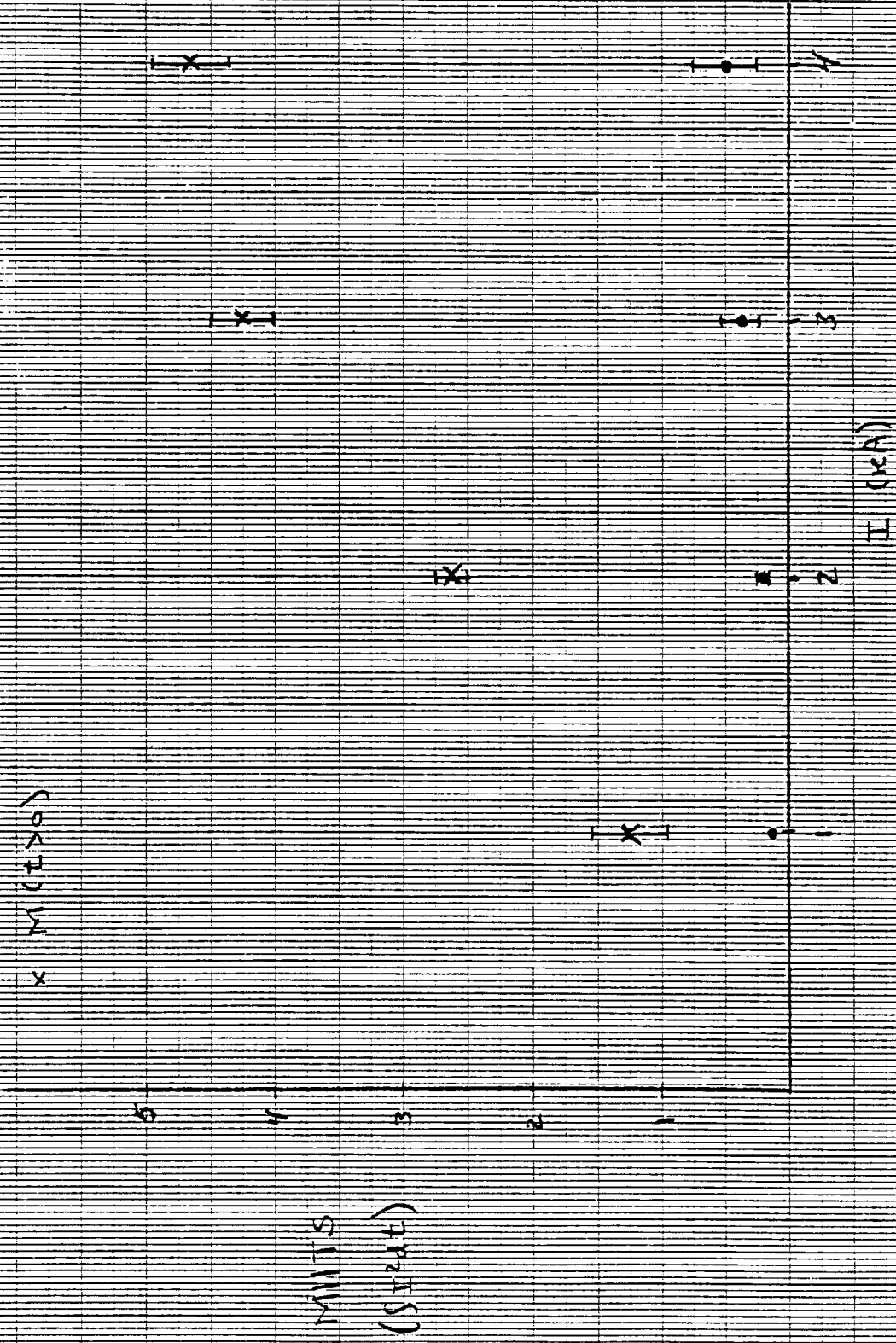
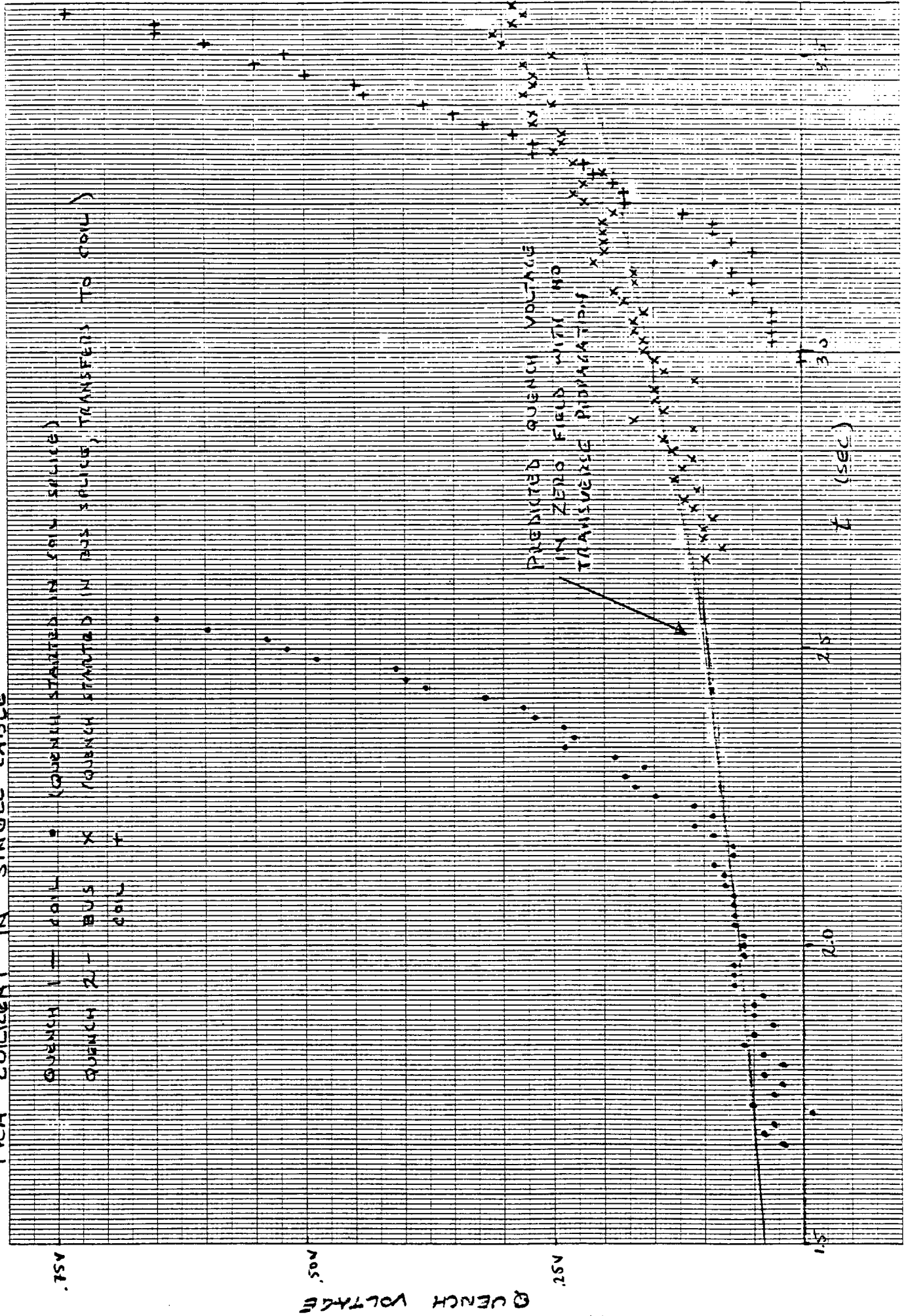


FIGURE 7

1 KA CURRENT IN SINGLE CABLE



2 KA CURRENT IN SINGLE CABLE

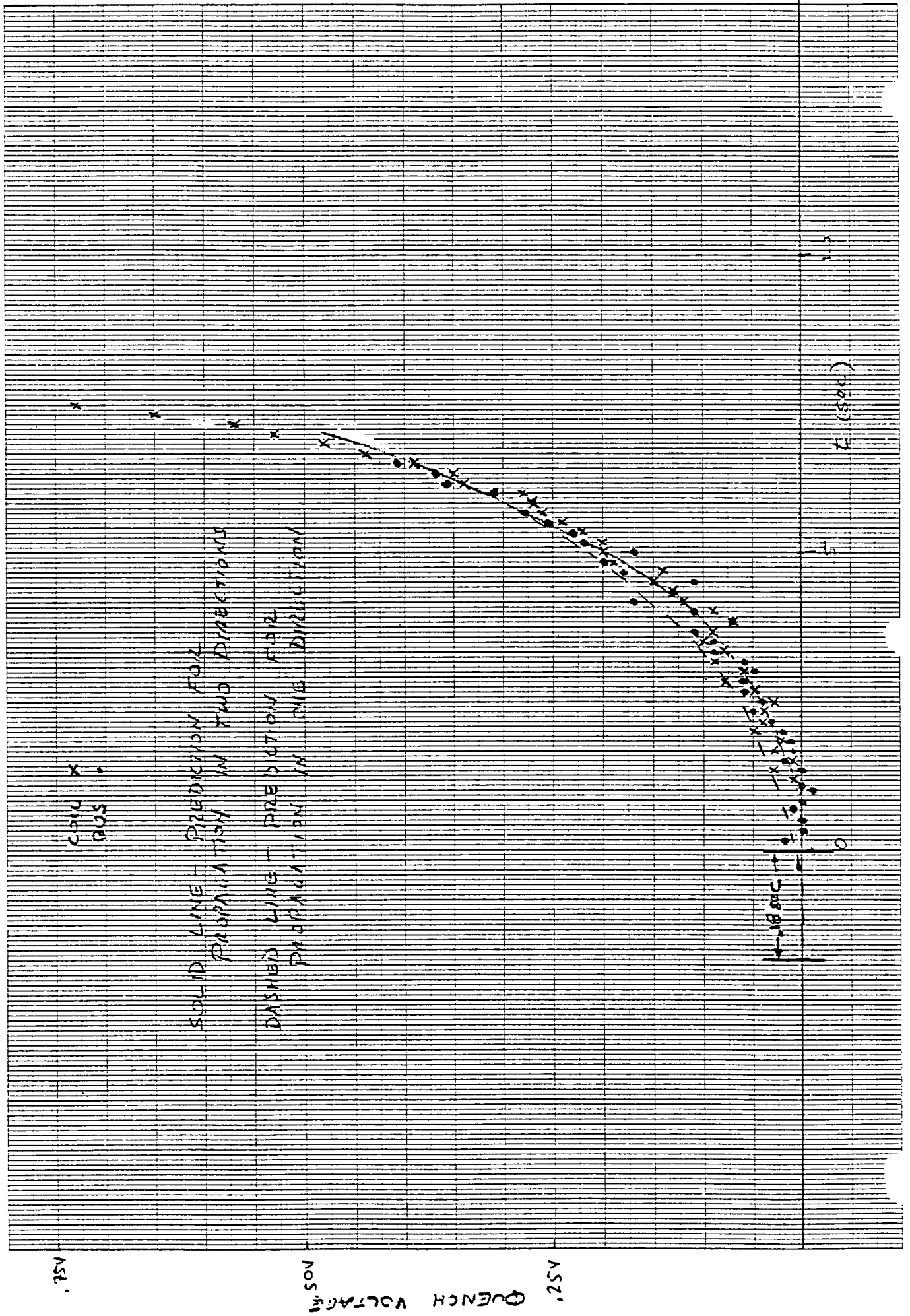


FIG 2E 9

3KA CURRENT IN SINGLE CABLE

COIL X
BUS -

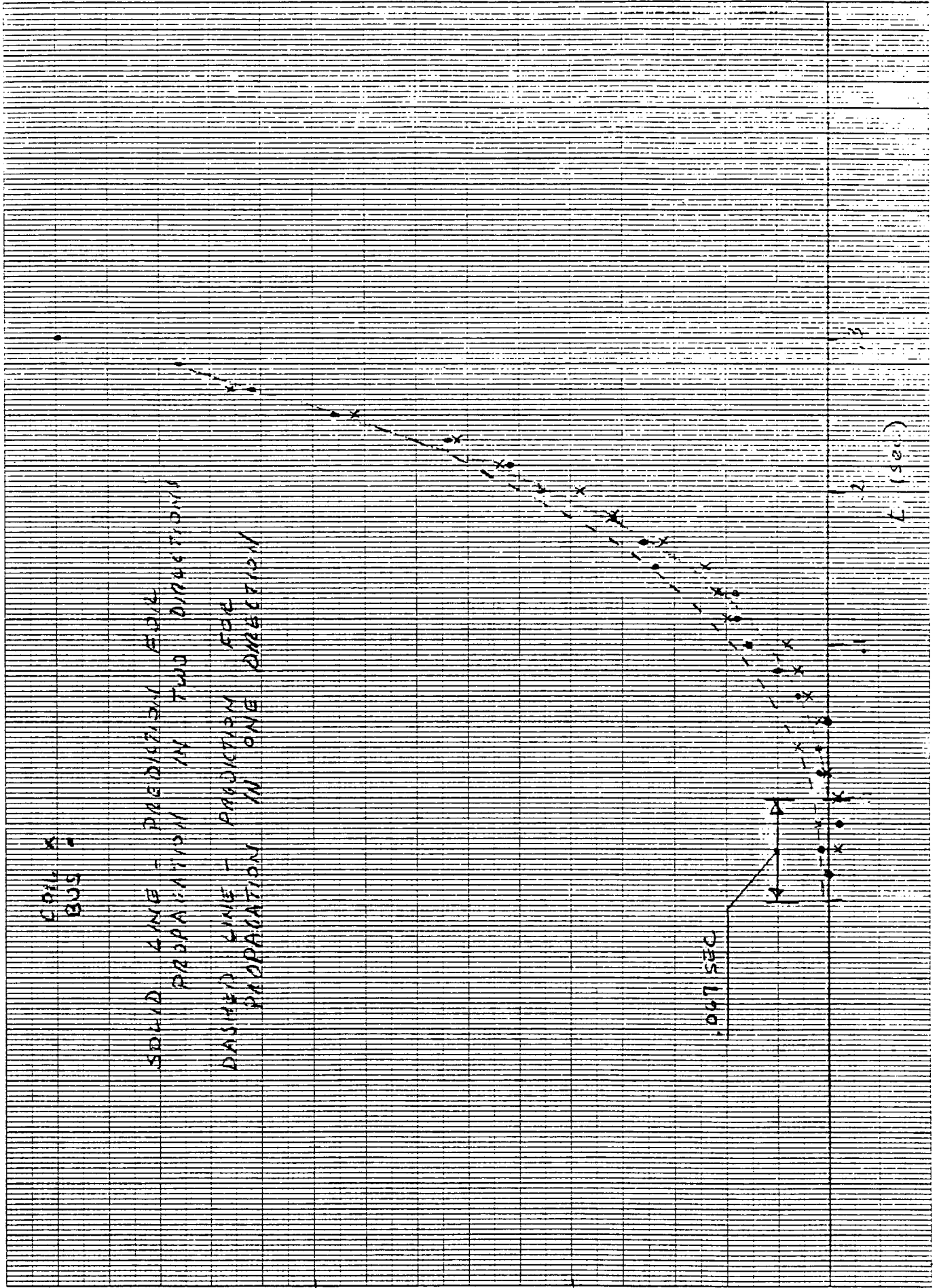
SOLID LINE - PROPAGATION FOR
PROPAGATION IN TWO DIRECTIONS

DASHED LINE - PROPAGATION FOR
PROPAGATION IN ONE DIRECTION

0.25V
0.50V
QUENCH VOLTAGE

0.067 SEC
0.199

t (sec)



1-KA CURRENT IN SINGLE CABLE

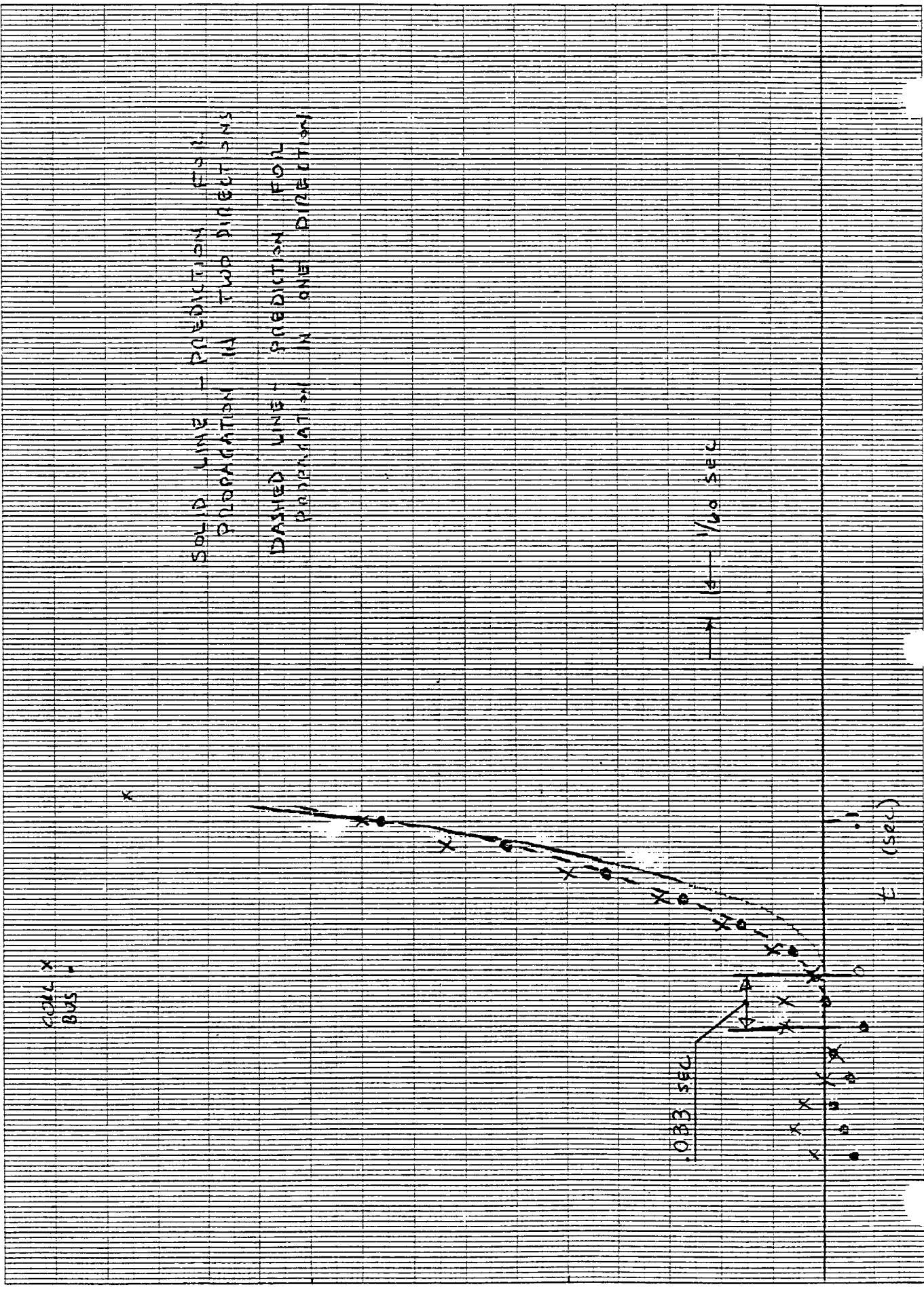


FIGURE 11

2KA - DOUBLE CABLE

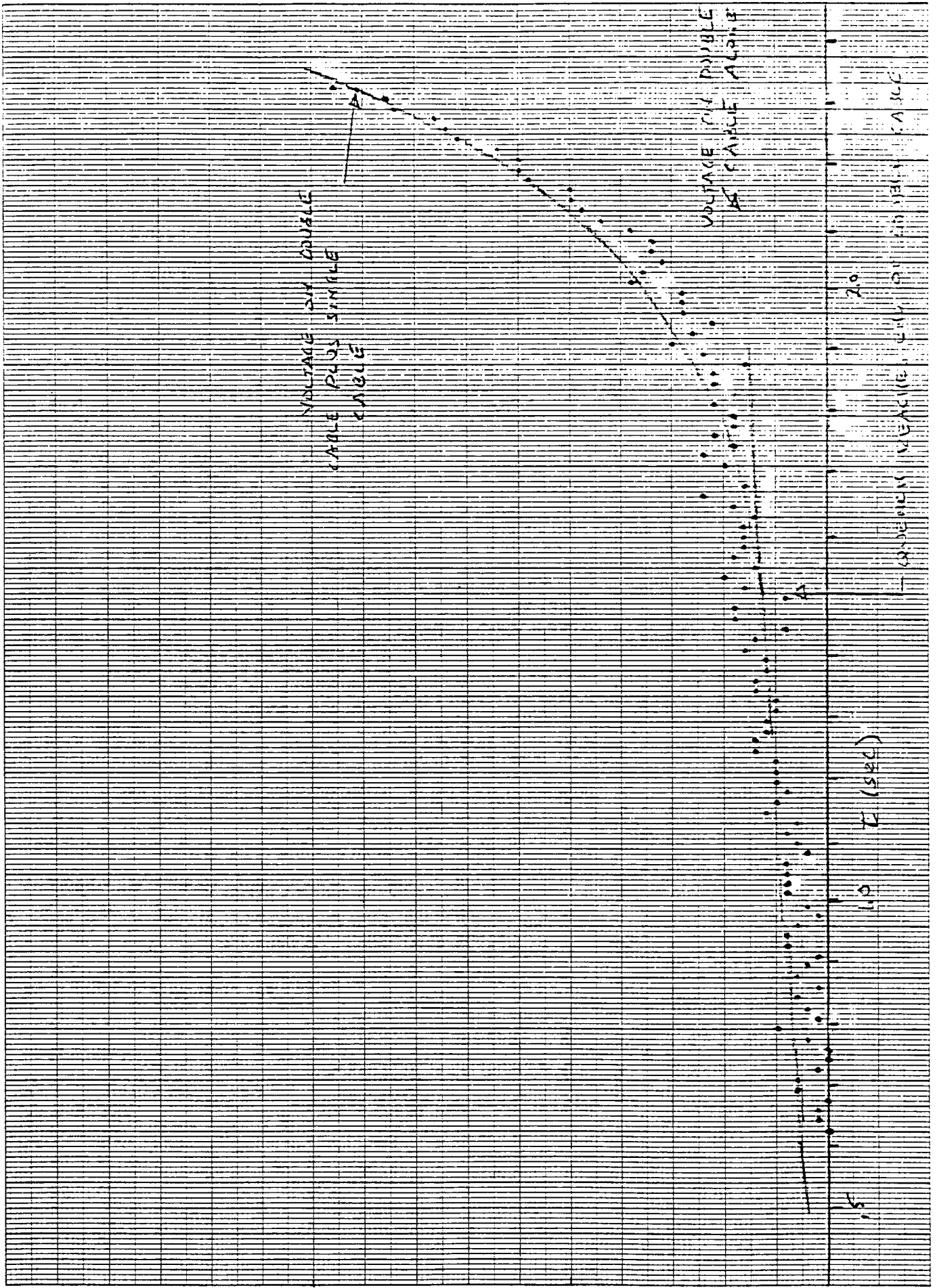


FIGURE 12

3 KA - DOUBLE CABLE

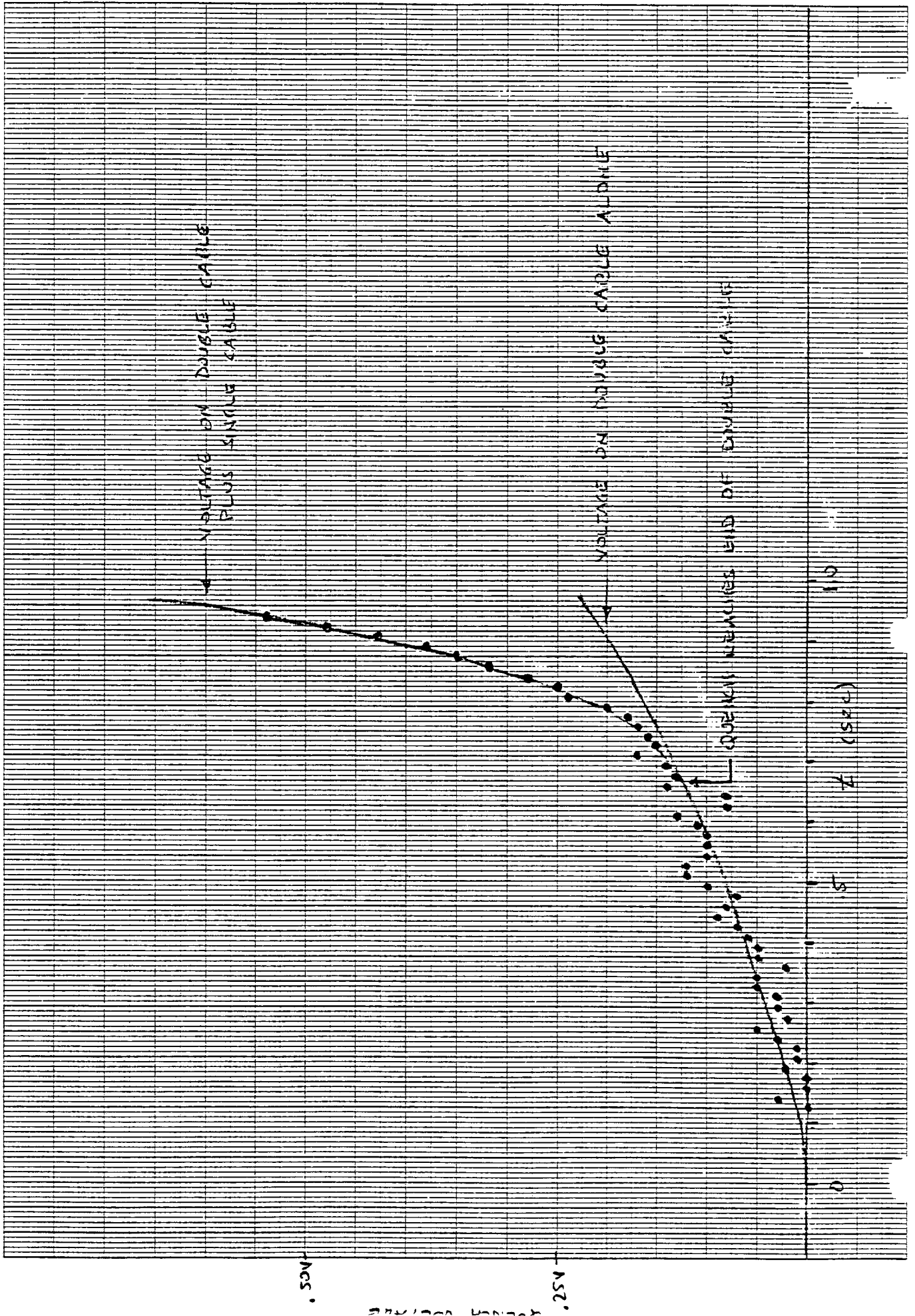


FIGURE 3

4 KA - DOUBLE CABLE

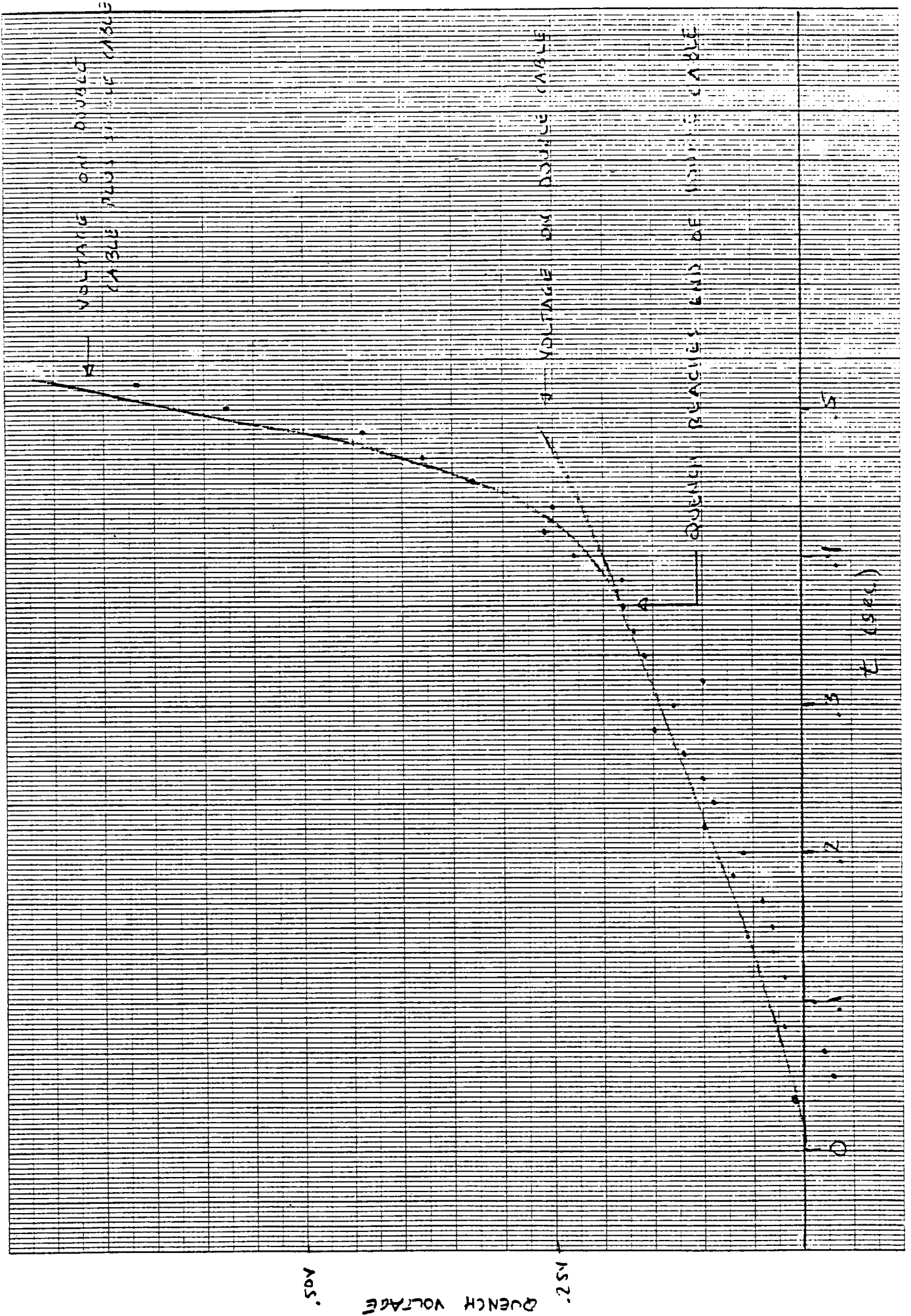
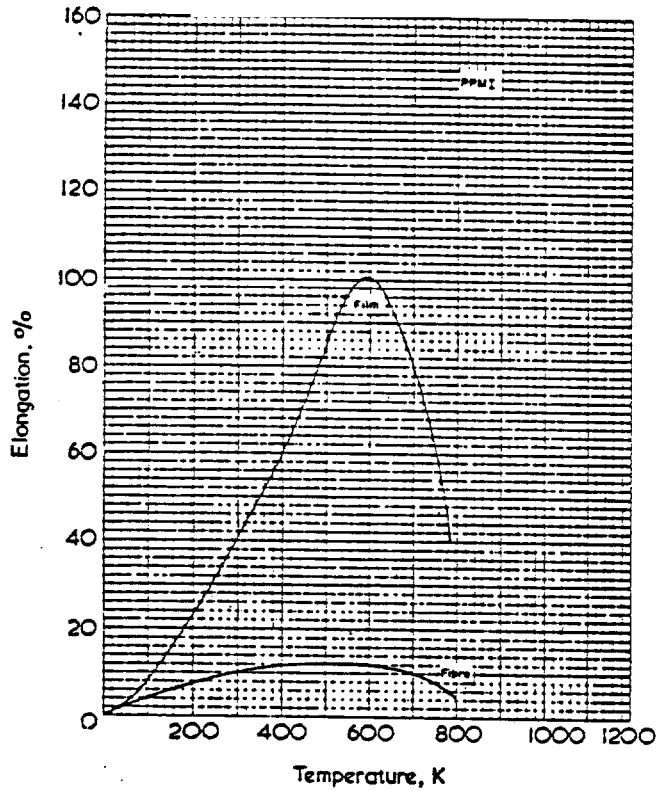
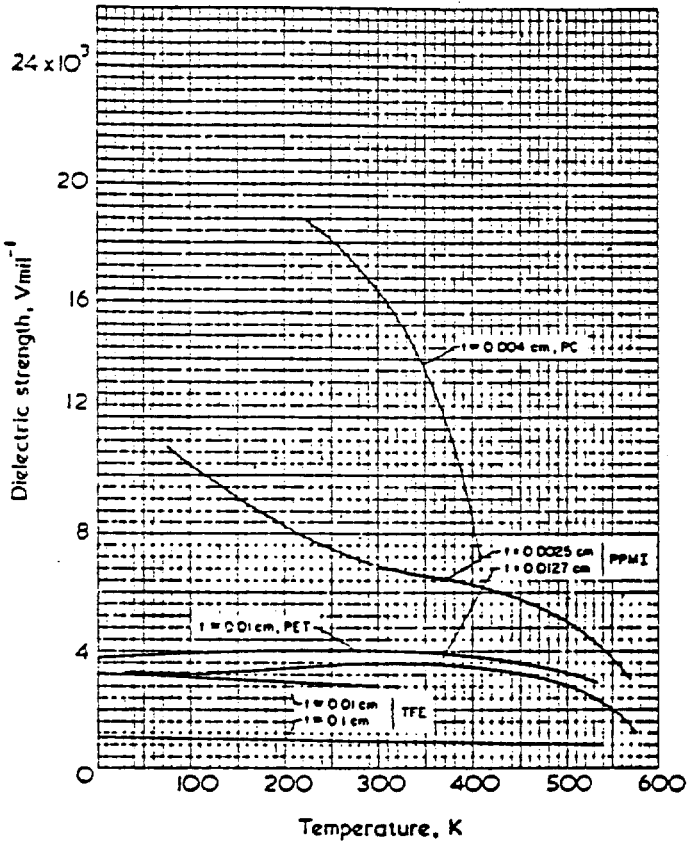


FIGURE 14



KAPTON H FILM IS A TRADE NAME FOR POLYPYROMELLITIMIDE (PPMI)

FROM: MECHANICAL, THERMAL AND ELECTRICAL
 PROPERTIES OF SELECTED POLYMERS,

BY R.P. REED, R.E. SCHRAMM AND A.F. CLARK,
 NATIONAL BUREAU OF STANDARDS

CRYOGENICS, FEB. 1973

FIGURE 15